OPEN ACCESS

Multiplexed endoscopic imaging of Barrett's neoplasia using targeted fluorescent heptapeptides in a phase 1 proof-of-concept study

Jing Chen ,[1] Yang Jiang,[2] Tse-Shao Chang,[3] Bishnu Joshi,[1] Juan Zhou,[1] Joel H Rubenstein,[1] Erik J Wamsteker,[1] Richard S Kwon,[1] Henry Appelman,[4] David G Beer,[5] Danielle K Turgeon,[1] Eric J Seibel,[6] Thomas D Wang [1,3,7]

► Additional material is published online only. To view, please visit the journal online (http://dx.doi.org/10.1136/gutjnl-2020-322945).

[1]Internal Medicine, University of Michigan, Ann Arbor, Michigan, USA
[2]Biomedical Engineering, University of Washington, Seattle, WA, USA
[3]Mechanical Engineering, University of Michigan, Ann Arbor, Michigan, USA
[4]Pathology, University of Michigan, Ann Arbor, Michigan, USA
[5]Thoracic Surgery, University of Michigan, Ann Arbor, Michigan, USA
[6]Mechanical Engineering, University of Washington, Seattle, WA, USA
[7]Biomedical Engineering, University of Michigan, Ann Arbor, MI, USA

Correspondence to
Dr Thomas D Wang, Internal Medicine, University of Michigan, Ann Arbor, MI 48109, USA; thomaswa@umich.edu

Received 28 August 2020
Revised 15 September 2020
Accepted 17 September 2020
Published Online First 7 October 2020

Check for updates

To cite: Chen J, Jiang Y, Chang T-S, *et al*. *Gut* 2021;**70**:1010–1013.

MESSAGE

Improved methods for early cancer detection arising from Barrett's oesophagus (BE) are still needed. Imaging molecular expression patterns in BE patients can target neoplasia. We demonstrate a multiplexed fluorescence imaging approach to detect premalignant lesions with two fluorescently labeled heptapeptides specific for EGFR and ErbB2. Twenty-two BE patients underwent endoscopic imaging with a multimodal scanning fiber endoscope (mmSFE). In this pilot study, 92% of neoplastic lesions could be imaged by comparison with pathology, with only 11% false positives. This first-in-human study demonstrates feasibility to concurrently detect multiple targets in vivo and potential for early detection of cancers that are molecularly heterogeneous.

INIEDMORE DETAIL

Background

Oesophageal adenocarcinoma (EAC) is a deadly disease that has increased dramatically in incidence over the past several decades.[1 2] Endoscopic screening with white light illumination and random biopsy is limited by sampling error.[3] Dysplasia often presents with flat architecture and patchy distribution.[4] EGFR and ErbB2 are transmembrane tyrosine kinase receptors that stimulate epithelial cell growth, proliferation and differentiation.[5] Overexpression of these targets reflects a higher risk for cancer progression.[6–8] Multiplexed imaging methods take advantage of the broad spectrum of light over the visible and near-infrared (NIR) regimen. We aim to demonstrate clinical feasibility to visualise EGFR and ErbB2 expression simultaneously in vivo to detect Barrett's neoplasia.

Methods

Consecutive patients referred for either evaluation or therapy of Barrett's neoplasia were recruited for the study (NCT03589443). An mmSFE was designed to collect multiplexed fluorescence images concurrently. Target/background (T/B) ratios were calculated for each fluorescence image. More details on the methods and the multiplexed imaging technology can be found in the online supplemental file.

Results

The peptide QRHKPRE specific for EGFR was labelled with Cy5 via a GGGSK linker, (figure 1A).[9] KSPNPRF, specific for ErbB2, was labelled with IRDye800 via a GGGSC linker (figure 1B).[10] These fluorophores were chosen to minimise overlap between absorbance and emission spectra (figure 1C). The characteristics and stability of fluorescently labelled peptides are shown in online supplemental tables S1–S4. The pharmacology/toxicology study shows no acute adverse effects in animals (online supplemental tables S5 and S6). The phase 1 safety study was performed in n=25 human, and no abnormalities were identified in the laboratory results, urinalysis and ECG for either peptide, and no adverse events were found.

The mmSFE was designed to collect multiplexed fluorescence images (figure 1D–H). Contrast agents were administered, and real-time images were collected from n=22 subjects, table 1 (online supplemental videos S1–S23). Representative white light images are shown for squamous (SQ) and non-dysplastic BE (NDBE) (figure 2A,B). Minimal background was seen following peptide administration. Fluorescence images were collected in separate channels, and coregistered reflectance provided anatomic landmarks for image interpretation. A representative set of in vivo images for HGD and EAC is shown (figure 2C,D). Increased fluorescence intensities were seen from regions of HGD and EAC, and were confirmed by pathology. Immunohistochemistry (IHC) was performed to validate expression of EGFR and ErbB2 on excised specimens (online supplemental figure S1).

The T/B ratios using QRH*-Cy5 and KSP*-IRDye800 were measured from individual patients (figure 3A,B). For SQ (n=2) or NDBE (n=3), a mean (±SD) T/B ratio of 1.28±0.07 for QRH*-Cy5 and 1.33±0.15 for KSP*-IRDye800, respectively, was calculated. The T/B for (n=4) LGD was 1.23±0.05 and 1.18±0.10, respectively. For HGD (n=7) and EAC (n=6), a mean (±SD) T/B ratio of 1.61±0.21 and 1.68±0.24, respectively, was found. Leave-one-out cross-validation (LOOCV) was used to classify results (online supplemental table S7). Support vector machine (SVM) and logistic regression (LR) provided the highest classification accuracy of 91%. The imaging results revealed n=12, 1, 8 and 1 true positives, false positives, true negatives and false negatives, respectively, resulting in 92% sensitivity and 89% specificity. The decision

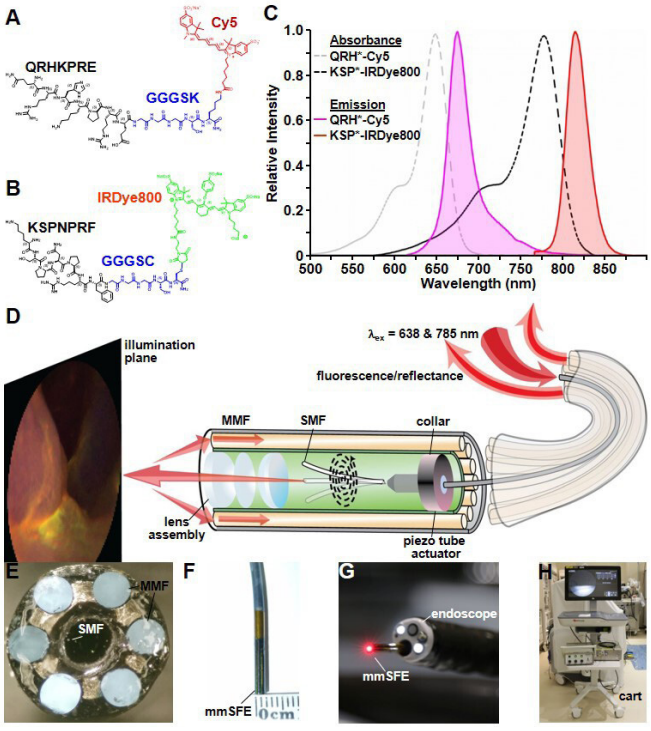

Figure 1 Fluorescently labelled peptides for multiplexed imaging. Biochemical structures are shown for (A) QRH*-Cy5 and (B) KSP*-IRDye800. (C) Peak absorbance of QRH*-Cy5 and KSP*-IRDye800 occurs at abs=648 and 776 nm, respectively. Peak fluorescence emits at em=675 and 812 nm, respectively. (D) Schematic diagram for the multimodal scanning fibre endoscope (mmSFE) is shown. Excitation at ex=638 and 785 nm is delivered through a single-mode fibre (SMF) that is scanned in a spiral pattern by a piezo tube actuator. The beam is focused onto the tissue surface (illumination plane) by a lens assembly. (E) Fluorescence is collected by a ring of large core multi-mode fibres (MMF) mounted around the instrument periphery. (F) The dimensions of the rigid tip are 9 mm in length and 2.4 mm in diameter. (G) This instrument passes forward through the 2.7 mm working channel of a standard medical endoscope (Olympus #GIF-HQ190). (H) The system is contained within a portable cart.

Table 1 Patient demographics

Age	Gender	Prague/stage	Tissue sampling	Pathology
68	M	C0M0I0	EMR/biopsy	SQ
57	M	C0M0I0	biopsy	SQ
84	F	C0M0I9	biopsy	NDBE
60	M	C0M1	EMR/biopsy	NDBE
56	M	C1M3	EMR/biopsy	NDBE
57	M	C7M9	biopsy*	LGD
56	F	C0M1	biopsy*	LGD
80	F	C0M0I0	biopsy*	LGD
67	M	C0M0I7	EMR/biopsy	LGD
79	F	C0M2	biopsy	HGD
88	M	C0M3	EMR/biopsy	HGD
79	M	C0M1I1.5	EMR/biopsy	HGD
85	M	C12M13	biopsy	HGD
79	M	C4M5	biopsy	HGD
66	M	C0M0	biopsy	HGD
60	M	C9M10	biopsy	HGD
75	M	T3N1	biopsy	EAC
73	F	C0M0I2	EMR/biopsy	EAC
81	M	C10M10	biospy†	EAC
71	M	C9M12I13	EMR/biopsy	EAC
55	F	T1a	biopsy	EAC
64	F	C0M1	EMR/biopsy	EAC

Multiplexed images were collected in vivo from the distal oesophagus of n=22 patients with a mean (±SD) age of 70.0±10.8 years. SQ, NDBE and LGD were identified in a total of n=2, 3 and 4 subjects, respectively. HGD and EAC were found in n=7 and 6 subjects, respectively. Modified Prague classification includes length in centimetres of circumferential Barrett's oesophagus (C), maximal tongue (M) and any proximal island (I). These findings were confirmed by histopathology from either EMR or biopsy.

*No tissue sampling performed at time of fluorescence imaging. Pathology based on findings from the most recent pathological reports before and after the imaging procedure.

†A mass was found in the thoracic oesophagus and the tissue diagnosis was obtained prior to this exam.

EAC, oesophageal adenocarcinoma; EMR, endoscopic mucosalresection; HGD, high-grade dysplasia; LGD, low-grade dysplasia; NDBE, non-dysplasticBarrett's oesophagus; SQ, squamous.

boundaries using SVM and LR are shown. The ROC curves using these methods with LOOCV are displayed (figure 3C). A higher AUC was achieved with multiplexed detection versus either target alone from bootstrap (figure 3D).

Comments

Here, we demonstrate feasibility to detect Barrett's neoplasia endoscopically by imaging two targets concurrently in vivo. Fluorescently labelled peptides specific for epithelial growth factor receptor (EGFR) and epithelial growth factor receptor2 (ErbB2) were administered topically in the distal oesophagus of n=22 BE patients. With conventional white light illumination, structural abnormalities associated with Barrett's neoplasia appeared subtle. By comparison, spatial patterns of target expression were visualised with high contrast using fluorescence. Two laser excitation wavelengths were delivered concurrently through a single flexible optical fibre using a prototype-wide-field endoscope accessory. Adequate signal was collected by using large core, high numerical aperture fibres. The regions imaged were compared with histopathology of specimens excised via either endoscopic mucosal resection or biopsy. IHC of these specimens confirmed heterogeneous expression of EGFR and ErbB2.

To our knowledge, this study first demonstrates clinical application of multiplexed fluorescence imaging during endoscopy. Many cancers, including EAC, are molecularly heterogeneous, thus detection of multiple targets is likely to be needed for accurate clinical diagnosis. Mucosal abnormalities with non-specific features, such as nodularity, ulceration and irregularities, may not be relied on to accurately locate Barrett's neoplasia. Several medical societies recommend random 4-quadrant biopsies for EAC surveillance, but this sampling method is inefficient and has been poorly adopted by community physicians.[11] Molecular biomarkers can be highly specific for disease, and are expressed well before neoplastic lesions become grossly apparent. Endoscopic imaging strategies for detecting these targets in vivo can be used to guide and prioritise high risk regions for resection, reduce surveillance frequency, and minimise over diagnosis.

Recently, detection of dysplasia and early EAC in BE patients was demonstrated using an antibody specific for vascular endothelial growth factor A. Bevacizumab was originally developed for cancer therapy, and was repurposed for diagnostic imaging by labelling with IRDye800.[12] Compared with antibodies, peptides are smaller in size, have faster binding kinetics, and

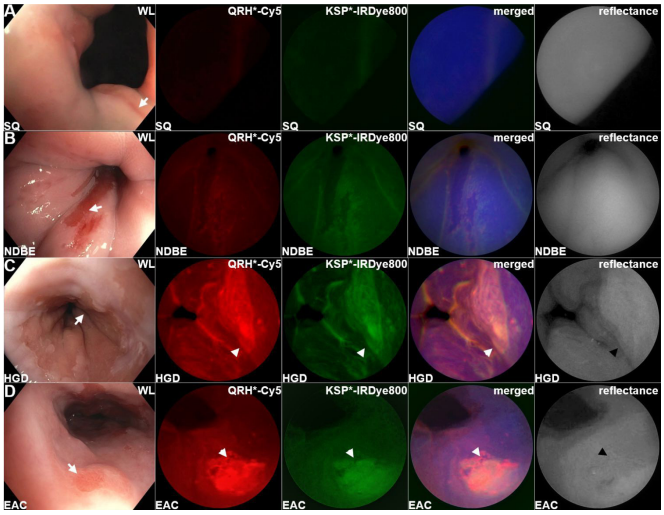

Figure 2 Barrett's oesophagus. Representative in vivo images collected endoscopically are shown from patients with (A) squamous (SQ), (B) non-dysplastic Barrett's oesophagus (NDBE), (C) high-grade dysplasia (HGD) and (D) oesophageal adenocarcinoma (EAC). The presence of NDBE is identified by the salmon red patches (arrows) in the white light images. Fluorescence images are collected after separate topical administration of QRH*-Cy5 and KSP*-IRDye800. The merged images show high contrast regions-of interest (ROI) where EGFR and ErbB2 (orange) are coexpressed. Coregistered reflectance images provide anatomical landmarks to interpret the location of the ROI's.

can be mass manufactured at lower costs.[13–15] The peptides were delivered to the mucosal surface in the distal oesophagus using topical administration. This method was effective for staining

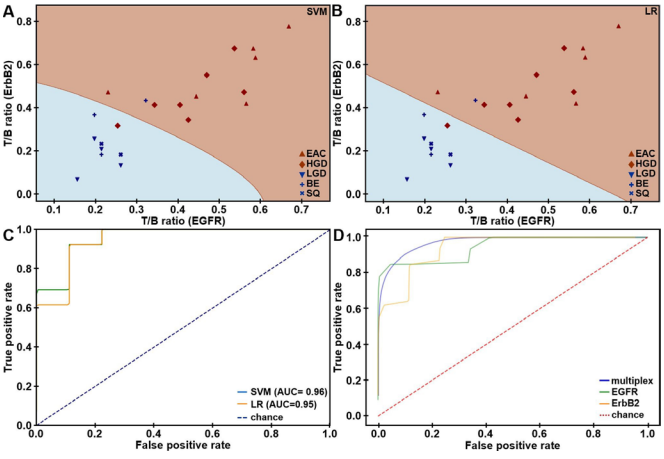

Figure 3 In vivo imaging performance. Scatter plot shows target/background (T/B) ratios measured for EGFR and ErbB2 expression in the fluorescence images collected in vivo from the distal oesophagus of n=22 patients. Decision boundaries show regions classified as either negative (blue) or positive (brown) for neoplasia using (A) support vector machine (SVM) and (B) logistic regression (LR) trained on all data. (C) ROC curves for classifying HGD/EAC from SQ/NDBE/LGD are shown using SVM and LR algorithms with leave-one-out cross-validation (LOOCV). (D) Average ROC curves from bootstrap using SVM (AUC=0.97) model trained on all data show that multiplexed detection provides improved performance than using either EGFR (AUC=0.95) or ErbB2 alone (AUC=0.94). AUC, area under curve; EGFR. epithelial growth factor receptor; ErbB2. epithelial growth factor receptor2; ROC, receiver-operator characteristic.

regions of neoplastic BE involvement.[16] Compared with systemic delivery, this approach localises the distribution of exogenous imaging agents to the target tissues only, minimises background and maximises image contrast. This strategy was chosen because the peptides used have similar binding kinetics.[9 10] Lectins have been investigated for detection of Barrett's neoplasia ex vivo,[17] but have not been demonstrated clinically. Fluorescently labelled peptides for targeted detection of premalignant lesions in the colon have also been shown clinically.[18 19] Folate has been developed for targeted imaging of ovarian cancer,[20] however, small molecules have limited flexibility for fluorescence labelling and would be difficult to use with multiplexed imaging.

In this work, light over a broad optical spectrum was collected using a flexible fibre endoscope accessory, and was separated into fluorescence and reflectance channels.[21] Multipixel photon counters with much higher sensitivity than the charge-coupled devices found in video endoscopes were used. Multiplexed detection was achieved by exciting Cy5 and IRDye800 at wavelengths with minimal overlap between the absorption and emission bands. Additional targets can be detected by extending this strategy to the full visible and NIR spectrum.[22] Fluorescence emission in the NIR regimen mitigates the effects of haemoglobin absorption and tissue scattering, and minimises tissue autofluorescence background.[23] The distal optics and scan strategy used provide much greater spatial resolution than an optical fibre bundle.

The clinical usefulness of this technology can be improved by addressing several study limitations. The peptides were administered separately to minimise potential binding interactions but can be combined to reduce time needed to reconstitute and prepare the peptides for delivery. After inserting the imaging accessory through the working channel, the fluorescence and HD-WLE images were not oriented. Accurate alignment would allow the fluorescence images to be more effective as a guide for tissue resection. This study was performed at a tertiary referral centre that specialises in treatment of patients with advanced BE, thus a cohort highly enriched with neoplasia was studied. Inclusion of more non-neoplastic subjects would better reflect the prevalence of disease seen in the community. In conclusion, we demonstrated a proof-of-concept study for detecting multiple targets concurrently in patients with Barrett's neoplasia and this strategy is promising for early detection of cancers in other hollow organs.

Acknowledgements We thank E Brady, D Chandhrasekhar, and A Cawthon for clinical support, and BR Reisdorph for regulatory support.

Contributors JC, BJ, JZ, DGB, DKT, EJS and TDW conceived and designed the experiments. JC, T-SC, JHR, EJW and RSK performed the experiments. JHR, YJ and EJS contributed to image and data analysis. HA reviewed pathology. JC, YJ, EJS and TDW wrote the manuscript.

Funding This study was supported in part by the National Institutes of Health U54 CA163059 (DGB, JHR, EJS, TDW), U01 CA189291 (TDW) and R01 CA200007 (EJS, TDW).

Competing interests None declared.

Patient consent for publication Not required.

Provenance and peer review Not commissioned; externally peer reviewed.

ORCID iDs
Jing Chen http://orcid.org/0000-0001-8863-2843
Thomas D Wang http://orcid.org/0000-0001-9182-9620

REFERENCES

1 Thrift AP, Whiteman DC. The incidence of esophageal adenocarcinoma continues to rise: analysis of period and birth cohort effects on recent trends. *Ann Oncol* 2012;23:3155–62.
2 Siegel RL, Miller KD, Jemal A. Cancer statistics, 2016. *CA Cancer J Clin* 2016;66:7–30.
3 Sharma P, Savides TJ, Canto MI, *et al*. The American Society for gastrointestinal endoscopy PIVI (preservation and incorporation of valuable endoscopic innovations) on imaging in Barrett's esophagus. *Gastrointest Endosc* 2012;76:252–4.
4 Spechler SJ, Sharma P, Souza RF, *et al*. American gastroenterological association technical review on the management of Barrett's esophagus. *Gastroenterology* 2011;140:e18–52.
5 Citri A, Yarden Y. EGF-ERBB signalling: towards the systems level. *Nat Rev Mol Cell Biol* 2006;7:505–16.
6 Dulak AM, Schumacher SE, van Lieshout J, *et al*. Gastrointestinal adenocarcinomas of the esophagus, stomach, and colon exhibit distinct patterns of genome instability and oncogenesis. *Cancer Res* 2012;72:4383–93.
7 Dulak AM, Stojanov P, Peng S, *et al*. Exome and whole-genome sequencing of esophageal adenocarcinoma identifies recurrent driver events and mutational complexity. *Nat Genet* 2013;45:478–86.
8 Miller CT, Moy JR, Lin L, *et al*. Gene amplification in esophageal adenocarcinomas and Barrett's with high-grade dysplasia. *Clin Cancer Res* 2003;9:4819–25.
9 Zhou J, Joshi BP, Duan X, *et al*. EGFR overexpressed in colonic neoplasia can be detected on wide-field endoscopic imaging. *Clin Transl Gastroenterol* 2015;6:e101.
10 Joshi BP, Zhou J, Pant A, *et al*. Design and synthesis of near-infrared peptide for in vivo molecular imaging of HER2. *Bioconjug Chem* 2016;27:481–94.
11 Kariv R, Plesec TP, Goldblum JR, *et al*. The Seattle protocol does not more reliably predict the detection of cancer at the time of esophagectomy than a less intensive surveillance protocol. *Clin Gastroenterol Hepatol* 2009;7:653–8.
12 Nagengast WB, Hartmans E, Garcia-Allende PB, *et al*. Near-infrared fluorescence molecular endoscopy detects dysplastic oesophageal lesions using topical and systemic tracer of vascular endothelial growth factor A. *Gut* 2019;68:7–10.
13 Lee S, Xie J, Chen X. Peptides and peptide hormones for molecular imaging and disease diagnosis. *Chem Rev* 2010;110:3087–111.
14 Wu AM, Senter PD. Arming antibodies: prospects and challenges for immunoconjugates. *Nat Biotechnol* 2005;23:1137–46.
15 Conner KP, Rock BM, Kwon GK, *et al*. Evaluation of near infrared fluorescent labeling of monoclonal antibodies as a tool for tissue distribution. *Drug Metab Dispos* 2014;42:1906–13.
16 Sturm MB, Joshi BP, Lu S, *et al*. Targeted imaging of esophageal neoplasia with a fluorescently labeled peptide: first-in-human results. *Sci Transl Med* 2013;5:184ra161.
17 Bird-Lieberman EL, Neves AA, Lao-Sirieix P, *et al*. Molecular imaging using fluorescent lectins permits rapid endoscopic identification of dysplasia in Barrett's esophagus. *Nat Med* 2012;18:315–21.
18 Burggraaf J, Kamerling IMC, Gordon PB, *et al*. Detection of colorectal polyps in humans using an intravenously administered fluorescent peptide targeted against c-Met. *Nat Med* 2015;21:955–61.
19 Joshi BP, Dai Z, Gao Z, *et al*. Wide-field endoscopic imaging of sessile serrated adenomas with fluorescently-labeled peptide probe. *Gastroenterology* 2017;152:1002–13.
20 van Dam GM, Themelis G, Crane LMA, *et al*. Intraoperative tumor-specific fluorescence imaging in ovarian cancer by folate receptor-α targeting: first in-human results. *Nat Med* 2011;17:1315–9.
21 Savastano LE, Zhou Q, Smith A, *et al*. Multimodal laser-based angioscopy for structural, chemical and biological imaging of atherosclerosis. *Nat Biomed Eng* 2017;1:0023.
22 Miller SJ, Lee CM, Joshi BP, *et al*. Targeted detection of murine colonic dysplasia in vivo with flexible multispectral scanning fiber endoscopy. *J Biomed Opt* 2012;17:021103.
23 Ntziachristos V, Bremer C, Weissleder R. Fluorescence imaging with near-infrared light: new technological advances that enable in vivo molecular imaging. *Eur Radiol* 2003;13:195–208.